◆ Human Brain Mapping 30:47–58 (2009) ◆

Limbic Dysregulation is Associated With Lowered Heart Rate Variability and Increased Trait Anxiety in Healthy Adults

Lilianne R. Mujica-Parodi,[1,2*] Mayuresh Korgaonkar,[1] Bosky Ravindranath,[1] Tsafrir Greenberg,[1] Dardo Tomasi,[3] Mark Wagshul,[4] Babak Ardekani,[5] David Guilfoyle,[5] Shilpi Khan,[6] Yuru Zhong,[1] Ki Chon,[1] and Dolores Malaspina[7]

[1]*Department of Biomedical Engineering, Stony Brook University, Stony Brook, New York*
[2]*Department of Psychiatry, Stony Brook University, Stony Brook, New York*
[3]*Department of Medicine, Brookhaven National Laboratories, Brookhaven, New York*
[4]*Department of Radiology, Stony Brook University, Stony Brook, New York*
[5]*Center for Advanced Brain Imaging, Nathan Kline Institute for Psychiatric Research, Orangeburg, New York*
[6]*Department of Medicine, Stony Brook University, Stony Brook, New York*
[7]*Department of Psychiatry, New York University, New York, New York*

Abstract: Objectives: We tested whether dynamic interaction between limbic regions supports a control systems model of excitatory and inhibitory components of a negative feedback loop, and whether dysregulation of those dynamics might correlate with trait differences in anxiety and their cardiac characteristics among healthy adults. **Experimental Design:** Sixty-five subjects received fMRI scans while passively viewing angry, fearful, happy, and neutral facial stimuli. Subjects also completed a trait anxiety inventory, and were monitored using ambulatory wake ECG. The ECG data were analyzed for heart rate variability, a measure of autonomic regulation. The fMRI data were analyzed with respect to six limbic regions (bilateral amygdala, bilateral hippocampus, Brodmann Areas 9, 45) using limbic time-series cross-correlations, maximum BOLD amplitude, and BOLD amplitude at each point in the time-series. **Principal Observations:** Diminished coupling between limbic time-series in response to the neutral, fearful, and happy faces was associated with greater trait anxiety, greater sympathetic activation, and lowered heart rate variability. Individuals with greater levels of trait anxiety showed delayed activation of Brodmann Area 45 in response to the fearful and happy faces, and lowered Brodmann Area 45 activation with prolonged left amygdala activation in response to the neutral faces. **Conclusions:** The dynamics support limbic regulation as a control system, in which dysregulation, as assessed by diminished coupling between limbic time-series, is associated with increased trait anxiety and excitatory autonomic outputs. Trait-anxious individuals showed delayed inhibitory activation in response to overt-affect stimuli and diminished inhibitory activation with delayed extinction of excitatory activation in response to ambiguous-affect stimuli. *Hum Brain Mapp 30:47–58, 2009.*

Key words: fMRI; amygdala; anxiety; stress; time-series; prefrontal cortex; control systems; limbic; connectivity; dynamic; heart rate variability; autonomic; cardiac; homeostasis

Contract grant sponsor: the Office of Naval Research; Contract grant number: N0014-04-1-005; Contract grant sponsor: the National Institutes of Health; Contract grant number: 5-MO1-RR-10710; Contract grant sponsor: National Institutes of Health; Contract grant number: K24-MH01699.

*Correspondence to: Lilianne R. Mujica-Parodi, Director, Laboratory for the Study of Emotion and Cognition, Departments of Biomedical Engineering and Psychiatry, Health Sciences Center T18, State University of New York at Stony Brook, Stony Brook, NY 11794-8181. E-mail: lstrey@stonybrook.edu

Received for publication 31 August 2006; Revised 11 August 2007; Accepted 20 August 2007

DOI: 10.1002/hbm.20483

Published online 27 November 2007 in Wiley InterScience (www.interscience.wiley.com).

INTRODUCTION

Functional MRI studies have typically investigated the amplitude of activation in regions of interest (ROI); however, increasing interest has focused on the possibility of exploiting the dynamic components of the fMRI time-series to explore connectivity within the brain. While neuroscientists often speak anecdotally about brain "circuitry," there exists the exciting and largely unexplored possibility of using fMRI BOLD activation to quantify the strength of "excitatory" and "inhibitory" pathways, treating ROI time-series as signal inputs and outputs in a control systems model. A control system may be defined as "a collection of interconnected components that can be made to achieve a desired response in the face of external disturbances" [Khoo, 2000]. In the case of physiology, the desired response is not only excitatory, to address the external disturbance, but also inhibitory, to maintain homeostasis by bringing the system back to baseline. Within this context, "inhibitory" activation is not to be understood as "lack of activation," but rather reflects increase in BOLD signal of those ROIs that work to suppress the excitatory component of the circuit.

Control mechanisms are present at almost every level of physiology. At the molecular scale, the dynamics between potassium, chloride, and sodium ions regulate the action potential and its return to baseline [Hodgkin and Huxley, 1952]. At the level of neurotransmitters, antagonistic neuro-receptors provide the excitatory (glutamate) and inhibitory (GABA) components of a negative feedback loop that maintain homeostasis [Calabresi et al., 1991]. Equivalent regulatory mechanisms are present at other scales, such as that of the autonomic nervous system via interactions between sympathetic and parasympathetic components [Kandel et al., 2000], of the endocrine system via interactions between cortisol and DHEA [Charney, 2004], of the balance of glucose and insulin [Insel et al., 1975], and the maintenance of core body temperature via vasodilation [Heldman, 2003]. In a well-regulated control system, the excitatory and inhibitory components work closely together. Thus, in the absence of an environmental need for an extended excitatory response, the time-series describing the excitatory and inhibitory components should be highly correlated with minimum lag. This tight coupling results in dampening the impact of the chaotic external environment, or maintenance of homeostasis.

As shown by Figure 1, the excitatory and inhibitory components of the limbic system have, by now, been relatively well-mapped out in the animal literature [LeDoux, 2000; Maren, 2005], making the dynamic regulation between these regions a plausible candidate for control systems modeling. In spite of numerous parallel pathways within the system, the medial central nucleus of the amygdala forms the chief excitatory component of the arousal response [Davis and Whalen, 2001], with the lateral amygdala providing inhibitory modulation of the medial central nucleus, and the basal amygdala providing either positive modulation of the medial central nucleus (via direct pathways) or negative modulation of the medial central nucleus (via the intercalated nuclei) [Maren, 2005]. The primary inhibitory pathways, identified primarily by intracellular recording/lesion studies of fear extinction, are the medial prefrontal cortex [Baxter et al., 2000; Blair et al., 2005; Izquierdo and Murray, 2005; Izquierdo et al., 2005; Phelps et al., 2004; Rosenkranz et al., 2003; Sotres-Bayon et al., 2006] and the hippocampus—the latter hypothesized to provide a "context" for potentially aversive stimuli [Corcoran et al., 2005; Sotres-Bayon et al., 2004]. Two distinct models have been proposed for the interactions between the amygdala, medial prefrontal cortex, and hippocampus [Sotres-Bayon et al., 2004]. In the first ("Model A"), the hippocampus and the medial prefrontal cortex are modeled as two independent components that inhibit the activation of amygdala. In the second ("Model B"), the hippocampus is hypothesized to modulate the medial prefrontal cortex, which then inhibits the amygdala. For both Models A and B, limbic outputs from the amygdala project to the hypothalamus. The hypothalamus controls the autonomic nervous system, itself another negative feedback

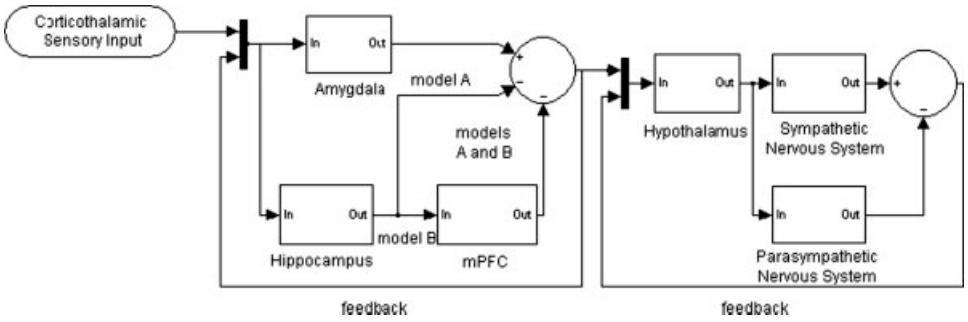

Figure 1.

Viewed as a control system, the limbic system acts a negative feedback loop, with excitatory (medial central nucleus of the amygdala) and inhibitory (medial prefrontal cortex, hippocampus) components that, when well-regulated, serve to respond to arousing stimuli and then rapidly return to baseline. Outputs from the limbic system provide inputs, via the hypothalamus, to the autonomic nervous system, itself another negative feedback loop with excitatory (sympathetic) and inhibitory (parsympathetic) components.

loop with excitatory (sympathetic) and inhibitory (parsympathetic) components [Kandel et al., 1991]. This same circuitry has been identified with anxiety disorders in the human as well [Cannistraro and Rauch, 2003].

Basic research in control systems physiology surgically isolates the feed-forward and feedback components of the circuit, thereby permitting separate quantification. Under normal circumstances, this is not possible with neural research on human subjects; therefore, one of the central challenges in using fMRI signals for control systems analysis is quantifying limbic dysregulation from a self-interacting, intact circuit. This challenge, of quantifying dysregulation from an intact circuit, has already been largely addressed for the autonomic nervous system by the development of newer methods of heart-rate variability analysis (HRV). Thus, approaches developed for HRV analysis may ultimately be of help in suggesting techniques for quantifying limbic dysregulation using fMRI.

HRV measures variability between successive heartbeats (R–R intervals), and is thought to reflect homeostatic regulation between sympathetic and parasympathetic components of the autonomic nervous system. Because certain pathological conditions, such as heart disease [Goldstein et al., 1975], hypertension [Abboud, 1982; Julius et al., 1975] and sudden cardiac death [Schwartz and De Ferrari, 1987], are accompanied by disruptions in the balance between these two components, HRV has received much attention within the cardiology literature as a potentially valuable noninvasive tool to detect and understand cardiac illness. HRV has historically developed from two separate and conceptually divergent approaches: the first quantifies dysregulation indirectly by deconvolving a complex waveform into its excitatory and inhibitory contributions, while the second quantifies dysregulation directly by calculation of the amount of "complexity" or "chaos" in the system. For both approaches, power is increased by typically collecting HRV data over 24-h; however, the measurements themselves reflect short-acting (0.04–0.50 Hz) autonomic regulation in response to environmental fluctuations.

Original work on HRV was focused on the first approach, via estimation of the power spectrum of instantaneous heart rate fluctuations [Akselrod et al., 1981; Pomeranz et al., 1985]. Using sympathetic and parasympathetic blockers, several bandwidths were identified as being particularly physiologically significant: frequencies between below 0.04 Hz (Very Low Frequency, or VLF); 0.04–0.15 Hz (Low Frequency, or LF); and 0.15–0.40 Hz (High Frequency, or HF) [Akselrod et al., 1981]. The VLF represents hormonal and temperature fluctuations, the LF represents both sympathetic and parasympathetic influences, and the HF represents parasympathetic contributions alone [Malik and Camm, 1993]. The ratio of the LF/HF spectrum was shown to provide a reasonable approximation of the sympathovagal balance, with high LF/HF indicating sympathetic dominance, and low LF/HF indicating predominantly vagal control.

In spite of the predictive value of the sympathovagal balance in predicting disease, the power spectrum density (PSD) method has not been widely accepted by cardiologists as a clinical instrument. This is predominantly because of a well-known deficiency in the PSD method: the LF bandwidth is not solely representative of the sympathetic influence [1996]; therefore a LF/HF ratio cannot be a precise measure of the balance between sympathetic and parasympathetic components. Moreover, the PSD method may be further compromised by the fact that the LF/HF ratio is linear, which cannot account for the significant nonlinear components of heart rate variability [Braun et al., 1998].

The principal dynamic modes (PDM) analysis of heart rate variability was developed to address the problem of more precisely separating out the sympathetic and parasympathetic components of heart rate variability, and is explicitly nonlinear. The PDM are calculated using Volterra–Wiener kernels based on expansion of Laguerre polynomials [Zhong et al., 2004]. Originally the method, applied to physiological systems, required both input and output signals [Marmarelis, 1997; Marmarelis et al., 1999; Marmarelis and Orme, 1993], although later work [Zhong et al., 2004] modified the method to include only a single output signal. Comparisons of PDM to PSD using sympathetic and parasympathetic blockers (atropine and propanolol) [Chon et al., 2006; Zhong et al., 2006; Zhong et al., 2004] have demonstrated that PDM is significantly more accurate than PSD in separating out the sympathetic and parasympathetic components of heart rate variability in humans.

The "nonlinear complexity with shannon entropy" method of HRV represents the second approach, that of directly quantifying dysregulation of a system by measuring the degree of complexity or chaos in the system [Kurths et al., 1995; Voss et al., 1995, 1996]. Symbolic dynamics is estimated by first binning R–R intervals into four groups, represented by "symbols" "0," "1," "2," and "3":

$$0:\ \mu < t_n - t_{n-1} \leq (1 + a)^*\mu$$
$$1:\ (1 + a)^*\mu < t_n - t_{n-1} \leq \infty$$
$$2:\ (1 - a)^*\mu < t_n - t_{n-1} \leq \mu$$
$$3:\ 0 < t_n - t_{n-1} \leq (1 - a)^*\mu$$

where $t_n - t_{n-1}$ = R–R interval, μ = mean R–R interval, and $a = 0.1$. Each "word" is composed of combinatorial arrangements of the symbols, with three symbols per word. If the probability of occurrence of a word is less than a set threshold, in this case: 0.001, then the word is defined as a "forbidden word." Increased forbidden word count therefore indicates both decreased chaos in the system as well as lowered heart rate (R–R) variability. Shannon entropy, a measure of chaos, is calculated as: $H_k = \sum_{W_k} p(\omega) \log_2 p(\omega)$ where W_k is the set of all words of length k and $p(\omega)$ is the probability of occurrence of words.

Diagnoses of regulatory diseases typically involve testing by perturbing the system and then observing the dynamics by which the body returns to homeostasis; for example, by ingesting a bolus of glucose to screen for diabetes [Graci et al. 1999; Kernohan et al., 2003; Lucas et al.,

1986; Rolandsson et al., 2001] or a bolus of dexamethasone to screen for Cushing's disease [Sriussadaporn et al., 1996; Tyrrell et al., 1986]. Other diagnostic tests avoid the use of bolus inputs, but instead quantify dysregulation in terms of the degree of output chaos in response to mild and chaotic inputs. One such method is the nonlinear complexity with Shannon entropy method of calculating HRV [Voss et al., 1995] described earlier, which has shown promise in predicting risk for myocardial infarction [Bauernschmitt et al., 2004; Huikuri and Makikallio, 2001; Huikuri et al., 2003; Lombardi, 2002; Makikallio et al., 2002; Swynghedauw et al., 1997; Vigo et al., 2004; Voss et al., 1995, 1996]. By analogy, our results suggest the potential utility of using fMRI time-series as outputs in neural control systems, an approach that has been proven to be useful in modeling physiology, and which may also have practical applications in diagnosis—or even identification of vulnerability towards—stress-related disorders.

We hypothesized that individuals with greater trait anxiety were unable to maintain homeostasis of the neural emotional arousal response as effectively as their less-anxious colleagues, shifting the emphasis from an abnormal variable to an abnormal dynamic between the excitatory and inhibitory influences responsible for modulating one another. This would imply that vulnerability towards anxiety would be characterized by lowered cross-correlation between the functional activation of the excitatory and inhibitory limbic components of the emotional arousal response, while inversely, resilience towards anxiety would be characterized by heightened cross-correlation between these same limbic components. Moreover the dynamics of the data might themselves be able to shed light on the respective roles of the different limbic areas in modulating the arousal response and its effects on the excitatory (sympathetic) and inhibitory (parasympathetic) components of short-term cardiovascular regulation, measured via heart rate variability [Breiter et al., 1996]. Our long-range goal is to characterize limbic dysregulation using nonlinear transfer functions, the tools normally used for control systems analyses. However, given the ambitiousness of applying BOLD signals to control systems, for this preliminary study we had a more modest aim: to apply coarse-grained statistical techniques—specifically correlational analyses—to investigate whether there might be a relationship between limbic regulation, autonomic regulation, and trait anxiety. If so, then these preliminary findings would provide support for a more mathematically nuanced characterization of dysregulation, with potential utility in developing fMRI-based diagnostic tools for stress-related disorders.

MATERIALS AND METHODS

Participants

We recruited 65 healthy adult subjects into this study (28 men, 37 women; mean age = 26 year; SD = 8; max/min age = 18–49). A lengthy phone screening, as well as the scheduled clinical interview for DSM-IV [Ventura et al., 1998], were administered to rule out subjects with current or prior psychiatric illness. All subjects received a history and physical; subjects were excluded if they had a history of drug abuse, traumatic brain injury, cardiovascular illness (including high blood pressure), regular nicotine use, or any MRI exclusion criteria, including metal in the body, claustrophobia, or pregnancy/lactation. This study was approved by the Institutional Review Board of Stony Brook University, and all subjects provided informed consent.

Study Design, Tasks, and Stimuli

All subjects were hospitalized for 48 h at the Stony Brook University Hospital's General Clinical Research Center, to provide maximum control over the testing environment. Subjects were admitted to the hospital at 8 P.M., provided informed consent, and received a physician-administered history and physical to ensure eligibility in the study. The morning after the first night, subjects were asked to complete the state-trait anxiety inventory [Spielberger, 1983], an instrument that provides a psycho–social assessment of anxiety in healthy adults. Starting at 10:30 A.M., subjects then received ambulatory cardiac monitoring for the next 24 h until 10:30 A.M. the second day. At this point, subjects received an MRI.

While in the MRI scanner, the subjects underwent two runs of a blocked design fMRI task. The stimuli used for this task consisted of black and white pictures of male and female faces depicting anger, fear, happy, and neutral emotions [Ekman, 1993], which are known to reliably activate a limbic response [Phillips et al., 1997; Williams et al., 2004]. Subjects passively viewed the stimuli during scanning using an angled mirror mounted on the head coil and a screen placed directly outside the magnet bore. Stimuli were presented using a computer running E-prime software (version 1.0; Psychology Software Tools, Pittsburgh, PA) and were projected on to the screen using a projector placed outside the scanner room. The fMRI task consisted of blocked presentations of faces alternating with a 20 s fixation cross block, during which a white cross-hairs was presented on a black background ("Rest" block). Each fMRI run lasted for 5 min and 40 s and included two blocks of angry, neutral, happy, and fearful faces. Each face block consisted of nine different faces of the same emotion type, displayed for 2.2 s each for total block duration of 20 s.

Image Acquisition and Analyses

Image acquisition

Subjects were scanned on a 1.5T Philips Intera MRI scanner at the Stony Brook Hospital using a SENSE head coil. We chose to use a lower field strength, rather than the more standard 3T, to minimize susceptibility artifacts in the amygdala [Krasnow et al., 2003], while permitting

whole-brain acquisition for time-series. These were acquired using two blocks (one for each fMRI run) of 136 T2*-weighted echoplanar single-shot images covering the frontal and limbic areas of the brain, with TR = 2,500 ms, SENSE factor = 2, TE = 45 ms, Flip angle = 90° Matrix = 64 × 64, 3.9 × 3.9 × 4 mm^3 voxels, and 30 contiguous oblique coronal slices. In addition to the functional scan, an anatomical scan to match the slice orientation of the functional scan was obtained. The acquisition parameters for this sequence were: TR = 15 ms, TE = 450 ms, Matrix = 256 × 256, FOV = 250 and 30 contiguous oblique coronal slices with 4 mm slice thickness and no gap between the slices. The anatomical data were used to generate a customized EPI template to normalize our EPI scans to the standard frame of reference. The subject's head was secured with tape to minimize head movements during the scans.

Image analyses

The fMRI data analyses were performed using the Statistical Parametric Mapping software (SPM99) [Friston, 1995]. The raw functional BOLD images were first realigned to the first volume to remove movement-related artifacts using a sinc interpolation. The motion correction algorithm in the SPM99 software package is capable of correcting for motion within 3 mm. Movement for 59 of the subjects was found to be within 3 mm in each of the functional runs and was fully corrected. The other six subjects had motion ranging from 4–5 mm and were therefore only partially corrected. Removing these latter subjects did not affect the analyses, nor was motion found to be correlated with trait anxiety; therefore results for all 65 subjects were included in our reported results. Realigned images were then spatially normalized into 3 × 3 × 3 mm^3 using an affine transformation with a set of 7 × 8 × 7. Basis functions and a customized template that was created using the data for the first 12 subjects; the incomplete brain coverage and oblique nature of our slices required us to use a custom template for normalization. For each subject, the scalp was removed from a low-resolution EPI image, using the Brain Extraction Tool (BET) [Smith, 2002] available in MRIcro software, at a fractional intensity threshold of 0.5. These skull stripped images were then registered and normalized to each other and the average image was smoothed with a Gaussian kernel of 8 mm full-width half maximum and registered to the EPI template provided by SPM99 to generate the final template. The realigned and normalized time series were then smoothed with a Gaussian kernel of 8 mm full-width half maximum.

All statistical analyses employed during image processing were performed using the general linear model in SPM99. We used a boxcar design with four conditions (anger, fear, happy, and neutral) convolved with the canonical hemodynamic response function. Contrast images for each comparison, i.e., angry–neutral, fear–neutral, happy–neutral, neutral–rest, angry–rest, fear–rest, and happy–rest, were generated for each subject. We also generated T-statistic images for each of these contrasts. A random effects analysis was performed using a one-sample *t*-test with the fixed effects single subject level contrast images. All assessments at the group level were done after applying a Bonferroni correction for multiple comparisons. Only those voxels which passed the significance level of $P = 0.05$ were used to display the brain activations.

To evaluate the cross-correlation of BOLD responses in specific brain areas, we first defined ROI. For the amygdala and hippocampus, which are functionally known to be associated with the emotional arousal response, this was done a priori. Separate ROI masks for the left-right amygdala and the left-right hippocampus were traced on the standard T1 template provided with the SPM package, using established anatomical landmarks to delineate our ROI [Hastings et al., 2004]. These masks were then used to select the maximally-activated voxel to extract the individual subject time-series. Although using a single voxel may increase chances of false positives, we found that averaging the response in the entire ROI (only part of which may be maximally activated) distorted the time-series. For this reason, studies using time-series normally obtain them from single voxels, rather than averaged clusters [Nomura et al., 2004]. Given the lack of certainty regarding the specific functionally-relevant areas for the prefrontal cortex, we defined these ROIs post hoc. This was done by performing a random effects analysis over the entire subject population. Our results of the random effects analysis over 65 subjects showed two clusters centered in Brodmann areas 45 and 9 of the prefrontal cortex respectively, as well as bilateral activation in the amygdala and hippocampus (Fig. 2a–c). The maximally-activated voxel for each ROI was then selected and used to extract each individual subject's time-series. A check was done to validate if the voxel selected was within a cluster of at least three contiguous voxels. Voxels for 89% of all ROIs were within a cluster. Obtaining the time-series in this manner allowed us to exploit the advantages of both the single-voxel and cluster methods, which were optimized for signal and reliability, respectively.

We first extracted the time-course for the whole experiment for each ROI. Once the study design was convolved with the SPM hemodynamic response function, 11 signal values over the peristimulus intervals, defined from 2.5 to 30 s from the onset of each block, were obtained for each condition block. The signal values of all the rest conditions were averaged over the peristimulus interval and designated the baseline. We used this baseline to calculate the percentage signal change value for every timepoint in the peristimulus interval for all other condition blocks. Finally, we obtained peristimulus time-courses for each condition by averaging the percentage signal change over the peristimulus interval over all the blocks of that condition.

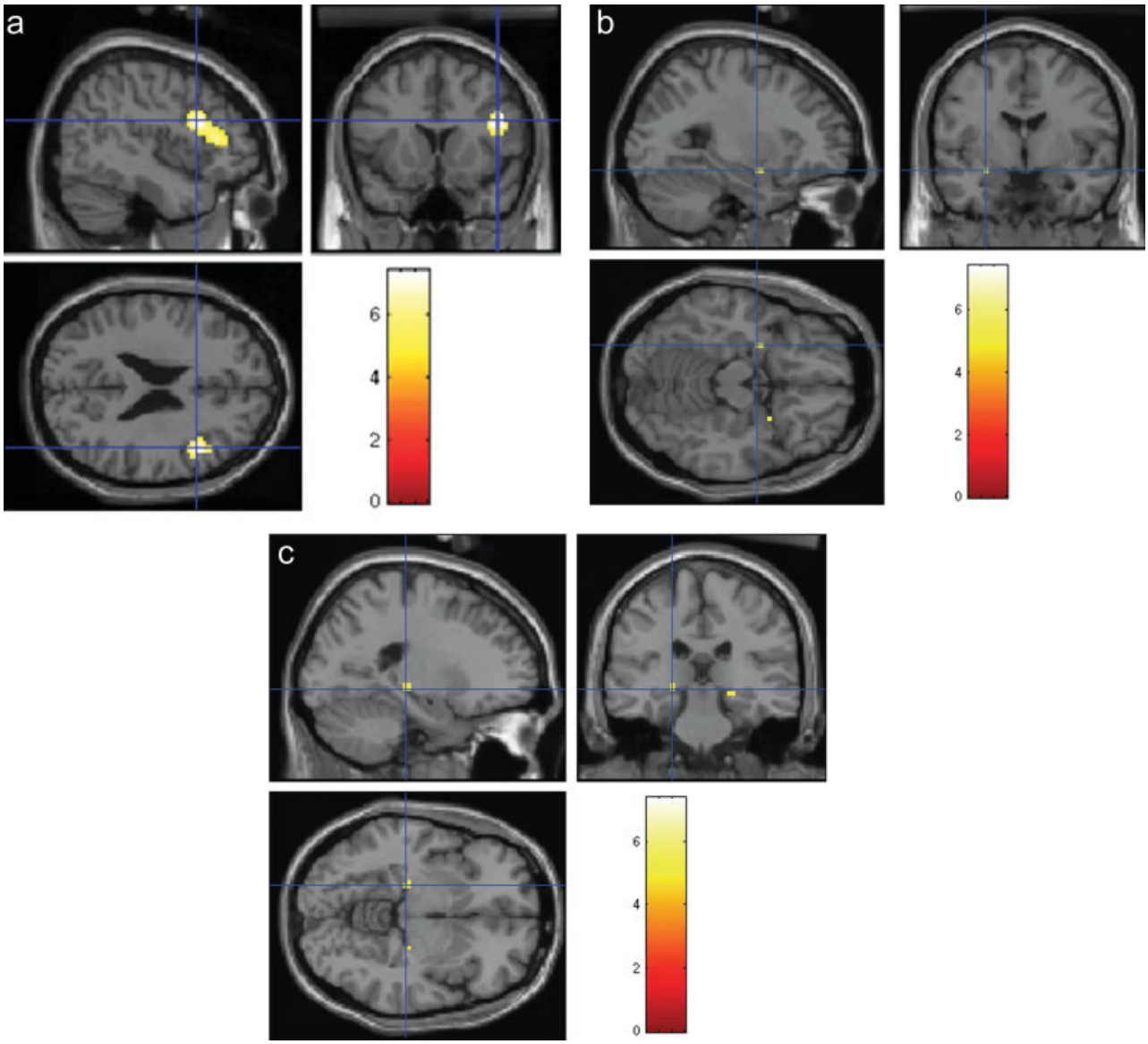

Figure 2.

BOLD activation maps of the random effects analyses for 65 healthy adults for neutral–rest contrast. (**a**) BOLD activation of Brodmann area 9 (−45, 15, 24; $t = 7.41$) and Brodmann area 45 (−54, 39, 3; $t = 7.16$) for neutral–rest contrast. (**b**) BOLD Activation of the right amygdala (27, −3, −15; $t = 5.06$) for neutral–rest contrast. (**c**) BOLD activation of the right (21, −27, −6; $t = 4.85$) and left (−24, −24, −9; $t = 5.34$) hippocampus for neutral–rest contrast.

Twenty-Four Hour ECG Acquisition and Wake Value Heart-Rate Variability Analyses

ECG acquisition

The subjects from whom we obtained the fMRIs were also monitored over 24 h with ECG; however, for this analysis we used only the wake values to avoid confounds because of different levels of REM activity. The signal was recorded using the Aria holter monitor (Del Mar Reynolds Medical, Irvine, CA) with a sampling rate of 128 samples/second. The records were then reviewed and edited using the Impresario Holter Analysis system (Del Mar Reynolds Medical, Irvine, CA). The ECG was manually reviewed to check for any misclassifications or errors. Identified erroneous R–R intervals were either replaced with values obtained by cubic spline interpolation or deleted depending upon the number of misclassifications. Participating subjects were asked to keep a log of their sleep and wake times and their 24 h data were separated according to their wake and sleep times. For subjects who failed to keep a

log, sleep, and wake times were approximated using their heart rate data. Wake and sleep times were confirmed using group mean changes in heart rate. Extracted R–R intervals were filtered using the adaptive filtering technique described by Wessel et al. [2000] (http://tocsy.agnld.uni-potsdam.de/ada.php) in order to remove artifacts and misclassifications that were not identified during the manual scan. The R–R intervals were converted to instantaneous heart rate with a sampling rate of 4 Hz [Berger et al., 1986; Kaplan], low-pass filtered at 0.5 Hz, down sampled to 1 Hz and zero-meaned. Fifteen of the original 65 subjects, from whom we obtained MRIs, were excluded because of either greater than 5% artifact in their ECG data or technical problems with the ECG. This left us with $n = 50$ for whom we had both usable fMRI and ECG data.

Heart-rate variability analyses

We performed our HRV analyses for wake periods using PDM [Chon et al., 2006] and nonlinear complexity with Shannon entropy [Voss et al., 1995] techniques.

General Statistical Analyses

We used the 11 data point time-series for left and right amygdala, left and right hippocampus, Brodmann Areas 9 and 45, and analyzed each of these six ROI over seven contrasts: neutral–rest, angry–rest, fear–rest, happy–rest, angry–neutral, fear–neutral, and happy–neutral. Given the problem of multiple-comparisons inherent in a statistical analysis with so many dependent variables, we employed a hierarchical strategy. We first performed a cross-correlational analysis as a gross measure of dysregulation (uncoupling between time-series) between all ROI pairs for all contrasts. This analysis narrowed down the primary contrasts of interest. This subset of contrasts was then analyzed for within-group differences with respect to: (a) time-series maximum values; and (b) values at each time-point in the time-series. The purpose of the secondary analyses was to provide an explanation for the relationships seen in the first, cross-correlational, analysis.

Cross-correlation is a standard measure of similarity between two signals, and therefore can function as a gross measure of dysregulation, since a well-regulated system with negative feedback should show coupled excitatory and inhibitory responses. For this analysis, lag was set to zero. Each subject produced 15 cross-correlation values (one for each possible pair of ROIs).

We used bivariate Pearson correlations to investigate the relationship between Trait Anxiety and limbic dysregulation for all three types of analyses (cross-correlations, maximum % signal change over the entire time-series, and maximum % signal change at each point in the time-series). Using bivariate Pearson correlations, we additionally investigated the relationship between limbic dysregulation (provided by the cross-correlation coefficients) and autonomic dysregulation (provided by wake HRV values using both the PDM and nonlinear complexity with Shannon entropy analyses).

Both components of our approach, the cross-correlations as well as the time-series, contributed to the large number of comparisons. Because we explicitly set out to take a dynamic approach, it was important to optimize temporal resolution. At the same time, greater temporal resolution required a greater number of comparisons, and therefore would also come at the cost of potential Type I errors. In awareness of this cost, we therefore performed the time-series analyses conservatively. To maintain the integrity of the 11 time-points while also down-sampling, we used a temporal cluster threshold, a sliding-window down-sampling technique akin to the spatial cluster thresholds that are often used to filter out single-voxel random noise in image processing. The threshold filtered out any isolated value, including only those that reached statistical significance at $P \leq 0.05$ for at least two consecutive points of the 11-point time-series. In spite of our attempts to ameliorate the problem wherever possible, the statistical problem of multiple-comparisons remains a significant limitation to the dynamic approach we took; therefore these results would best be viewed as exploratory, providing an estimation data set to be validated by future studies.

RESULTS

Trait Anxiety Ratings

The trait anxiety scale, like the characteristic it represents, is a continuous measure that in our sample of $n = 65$, provided a normal distribution (mean trait anxiety score = 38; SD = 10; max/min score = 21–67). Trait anxiety was not correlated with age, nor was it different for males and females. Using the hierarchical approach described in the Methods section, we compared the fMRI and trait anxiety levels using Pearson correlations for three types of dependent variables: (1) the cross-correlation coefficients r between all ROI-pairs; (2) the BOLD amplitude for each ROI; and (3) the BOLD time-series for each ROI.

Cross-Correlation Coefficients *r* Between All ROI-Pairs

For the cross-correlations between time-series for different ROIs, we found significant correlations for the neutral–rest, fear–rest, and happy–rest contrasts (Table I). In all cases, the greater the level of trait anxiety, the lower the limbic correlation coefficients (i.e., trait anxious individuals showed less coupling between their limbic time-series).

BOLD Amplitude for Each ROI

Correlational analyses, comparing trait anxiety and ROI activation for each of the contrast conditions defined by the cross-correlational analyses (neutral–rest, fear–rest, and happy–rest), found only one relationship between anxiety

TABLE I. Trait anxiety negatively correlated with cross-correlation coefficients *r* for region-of-interest pairs, suggesting diminished coupling between limbic components of negative feedback loops that modulate emotional regulation

Contrast	Cross-correlation pairs	Cross-correlation coefficient *trait anxiety (*r*)	Significance (*P*)
Neutral–rest	R Amygdala*L Amygdala	−0.30	0.02
	R Amygdala*BA45	−0.25	0.05
	L Amygdala*R Hippocampus	−0.29	0.02
	L Amygdala*L Hippocampus	−0.36	0.004
	L Amygdala*BA45	−0.27	0.03
	R Hippocampus*BA45	−0.29	0.02
Fear–rest	R Amygdala*BA45	−0.29	0.02
	L Amygdala*BA45	−0.26	0.04
	R Hippocampus*BA45	−0.30	0.02
	L Hippocampus*BA45	−0.33	0.007
Happy–rest	L Amygdala*BA45	−0.27	0.03
	R Hippocampus*BA45	−0.28	0.02
	BA45*BA9	−0.28	0.02

and activation amplitude of any of the ROIs for any of the contrast conditions. Individuals with higher trait anxiety showed less activation in BA45 for the fear–rest contrast ($r = -0.29$, $P = 0.02$).

BOLD Time-Series for Each ROI

For the sake of descriptive clarity, we will refer to the 30 s time-series (20 s block convolved with the hemodynamic response function) with respect to three time-periods: early (1–10 s), middle (11–20 s), and late (21–30 s) periods. We found significant correlations between trait anxiety and dynamic BOLD amplitude, particularly for the left amygdala and BA45 during the early and late periods. Trait anxious individuals, for the neutral–rest contrast, showed decreased early activation of BA45 (4–14 s; $-0.26 \leq r \leq -0.34$; $0.04 \leq P \leq 0.006$) and increased late activation of the left amygdala (23–27 s; $0.27 \leq r \leq 0.35$; $0.03 \leq P \leq 0.005$) (Fig. 3). For both fear–rest and happy–rest contrasts, trait anxious individuals also showed decreased early activation of BA45 (fear–rest: 4–16 s; $-0.25 \leq r \leq -0.32$; $0.03 \leq P \leq 0.009$; happy–rest: 10–14 s; $-0.25 \leq r \leq -0.28$; $0.04 \leq P \leq 0.02$). However, unlike the neutral–rest contrast, in response to the fearful and happy faces, trait anxious individuals showed increased late activation of BA45 (fear–rest: 23–27 s; $0.27 \leq r \leq 0.37$; $0.03 \leq P \leq 0.002$; happy–rest: 25–30 s; $0.30 \leq r \leq 0.50$; $0.02 \leq P \leq 0.000$) without an increase in late left amygdala activation. Post hoc analyses, of time-periods and ROIs identified above, confirmed a strong inverse relationship between early BA45 activation and late activation of the left amygdala in the neutral–rest contrast, with a peak inverse correlation at 8 s for BA45 and 26s for left amygdala ($r = -0.51$, $P = 0.000$) (Fig. 4); this relationship was not observed between late BA45 activation and late activation of the left amygdala. Inspection of the time-series suggested that the late left amygdala activation was not a lag in excitatory activa-

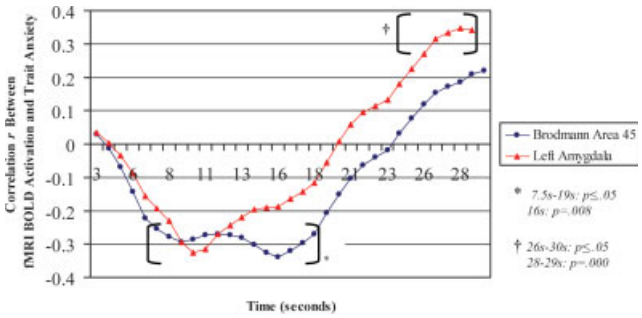

Figure 3.
Trait anxiety is associated with suppressed early BA45 BOLD activation and prolonged late left amygdala BOLD activation for neutral—rest contrast.

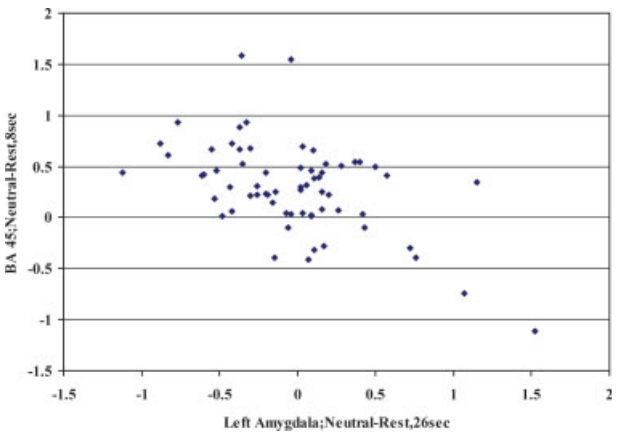

Figure 4.
Early (8 s) BA45 BOLD activation inversely correlates with late (26 s) left amygdala BOLD activation ($r = -0.51$;$P = 0.00$) for neutral—rest contrast.

tion, but rather prolonged activation that was already present; in effect, a delay in the response's extinction.

Higher fMRI Cross-Correlation Coefficients Correspond to Increased 24-h Heart Rate Variability

There was an inverse correlation between the cross-correlation coefficients for the neutral–rest contrast and sympathetic activation during the wake period; specifically: left amygdala versus BA 45 pair ($r = -0.27$, $P = 0.05$, $N = 50$). Supporting the above observation was the positive correlation, also for the neutral–rest contrast, between the cross-correlation coefficients and Shannon entropy (the amount of "chaos" in the heart rate) during wake periods; specifically: left amygdala versus BA 45 pair ($r = 0.36$, $P = 0.01$), left amygdala versus BA9 pair ($r = 0.36$, $P = 0.01$), left amygdala versus left hippocampus pair ($r = 0.31$, $P = 0.03$), left amygdala versus right amygdala pair ($r = 0.29$, $P = 0.04$) and left hippocampus versus BA45 pair ($r = 0.36$, $P = 0.01$).

Individuals with greater trait anxiety showed lower HRV as measured by waking nonlinear complexity with shannon Entropy ($r = -0.39$, $P = 0.005$, $N = 50$).

DISCUSSION

Our group analysis of 65 healthy adults confirmed the key roles of the bilateral amygdala, bilateral hippocampus, BA 9, and BA 45 in modulating emotional response in healthy adults. The cross-correlational analyses suggested that individuals with greater levels of trait anxiety show greater uncoupling, or dysregulation, of their limbic responses to the neutral, fearful, and happy faces. The time-series analyses narrowed the trait anxious individuals' limbic uncoupling further to a primary inverse relationship between suppressed early BA45 and heightened prolonged left amygdala activations in response to the affect-ambiguous (neutral) faces, and a delayed BA45 response without an increasingly prolonged left amygdala activation in response to the affect-overt (fearful and happy) faces.

That the affect-ambiguous, rather than the affect-overt, stimuli provoked a delayed extinction of the left amygdala response in trait anxious individuals, suggests that the most prominent feature separating the high anxiety from the low anxiety ends of the normal spectrum may not be the manner in which the excitatory components of the limbic system process threat, but rather how they process the potential for threat. These results are consistent with a number of patient studies [paranoid schizophrenia [Holt et al., 2006), borderline personality disorder [Donegan et al., 2003] showing that differences in neural activation as compared to controls occur predominantly in response to ambiguous, rather overtly affect-valent stimuli. Similar results were also found for a study of state anxiety in healthy controls [Somerville et al., 2004].

Studies that compared affect-ambiguous to affect-valent stimuli consistently found that the ventromedial [Shin et al., 2005; Williams et al., 2004], dorsolateral [Schienle et al., 2005], and orbitalfrontal [Schafer et al., 2005] prefrontal cortex were selectively activated during tasks that required discrimination of affect, suggesting that the prefrontal cortex may not only be inhibitory, but play a more specific role in threat assessment—amplifying or suppressing the arousal response depending upon whether threat is detected.

Development of increasingly sensitive ways to measure the dynamic interplay between BA45 and the left amygdala provides one possible manner to quantify limbic dysregulation. This approach is similar in basic philosophy to characterizing autonomic dysregulation via quantification of distinct excitatory and inhibitory components, as with the PSD and PDM methods of calculating heart rate variability. A contrasting manner of quantifying dysregulation is exemplified by the nonlinear complexity with Shannon entropy method of HRV analysis, which rather than referencing specific components of the system, quantifies instead a property (such as "chaos") of the system as a whole. This second type of approach is of little help mechanistically, since it provides only a very global measure of dysregulation, but it can be a powerful approach diagnostically once normative thresholds are set [Voss et al., 1996]. Our observation that time-series across excitatory and inhibitory ROIs become increasingly coordinated with increasing trait-calmness, and more and more chaotic with trait anxiety, is of the second type, and mathematical methods with increased sensitivity in quantifying chaos within the system, such as entropy, Lyapunov exponent and attractor dimension, may provide a fruitful direction for this research.

The ECG data show that *limbic* regulation in response to the affect-ambiguous stimuli, measured via cross-correlation coefficients between excitatory and inhibitory pathways (left amygdala * BA9, BA 45, left hippocampus), is correlated with autonomic regulation during wake periods, measured with two independent methods of HRV. Specifically, the results show that the higher the level of limbic dysregulation, the greater the waking sympathetic activation and the lower the waking "chaos" in the heart-rate. These two results are both consistent with one another and to be expected, since the inputs to the autonomic nervous system (itself a negative feedback loop between excitatory and inhibitory control) originate, via the hypothalamus, from the limbic outputs [Davis and Whalen, 2001; Kandel, 1991]. Since the external environment is chaotic, a well-regulated system will be able to modulate an excitatory (sympathetic) response with an equally strong inhibitory (parasympathetic) response at minimum lag, thereby maintaining homeostasis. As such, a well-regulated system will meet the demands imposed by the chaotic environment, but then quickly return to baseline—resulting in both a

lower average sympathetic activation during wake periods as well as higher chaos in the heart rate [in a dysregulated autonomic nervous system, the heart-rate shows less chaos because, once elevated, it remains elevated [Nahshoni et al., 2004; Poon and Merrill, 1997]. The use of a zero-lag cross-correlation therefore provides a likely explanation for why the coefficients obtained for the neutral, but not fearful or happy stimuli, were correlated with wake HRV. We would expect the greatest correlation between excitatory and inhibitory components of a negative feedback loop when the aim is for the system to respond and then quickly return back to baseline. This is most likely to occur in the absence of the need for sustained activation; i.e., stimuli that are initially ambiguous, and are then rapidly determined (by individuals at the trait-calm end of the normal spectrum) to be benign.

An expanding number of investigations have used fMRI to explore the neural mechanisms regulating autonomic arousal during cognitive, affective, and/or motor tasks [Critchley et al., 2005]. The role of limbic regions, particularly the anterior cingulate cortex (ACC), in autonomic regulation during challenging tasks has been repeatedly demonstrated, including modulation of cardiac activity [Critchley et al., 2003; Matthews et al., 2004]. Moreover, a recent study [Neumann et al, 2006] suggests that a genetic variation associated with both cardiac dysregulation and depressive symptoms also relates to corticolimbic brain activity during both cognitive/motor ("go/no-go") and emotional reactivity (face perception) tasks. The correlations between limbic and autonomic dysregulation also found in our study provide a possible bridge between fields in understanding a well-established body of research linking lowered HRV with emotional reactivity and mental illness. These include worry [Brosschot et al., 2006], generalized anxiety disorder [Gorman and Sloan, 2000; Wilhelm et al., 2001], panic disorder [Yeragani et al., 1998], depression [Davydov et al., 2006; Nahshoni et al., 2004; van der Kooy et al., 2006; Yeragani et al., 1991], and schizophrenia [Mujica-Parodi et al., 2005]; our results showing a correlation between trait anxiety and lowered HRV may reflect the same mechanism in a less severe form. Clearly, correlations alone do not imply causation. However, the known physiology between the limbic system and the autonomic nervous system (Fig. 1) do suggest the possibility that the emotional symptoms and lowered HRV seen in trait anxious individuals may be due to limbic outputs as a common cause. If so, then limbic dysregulation may be responsible for the lowered HRV seen in mentally ill patients as well.

CONCLUSIONS

Our results provide evidence for an association of trait anxiety with increased limbic dysregulation in response to both affect-ambiguous (Neutral) and affect-overt (fearful, happy) facial stimuli. Overall amplitude for the entire time-series did not show any relationship between trait anxiety and the excitatory components of the limbic system, but did show suppressed inhibitory activation in response to the fearful faces. However, analyses of ROI amplitude for each point in the time-series revealed different dynamics in response to affect-ambiguous and affect-overt stimuli. For the former, early (~8 s) inhibitory BA45 activation was strongly associated with suppression of late (~26 s) excitatory left amygdala activation; while for the latter, early inhibitory BA45 activation was also diminished, but showed heightened activation later in the time-series. We interpret these data as suggesting that trait anxious individuals may be impaired in their modulation of Brodmann Area 45 in detecting that a stimulus is not a threat, and therefore suppressing left amygdala activation. Analogously to the coarse-grained symbolic dynamic method of quantifying autonomic dysregulation, our cross-correlations between limbic regions suggested utility in quantifying limbic dysregulation. The more trait anxious the subject, the less correlated were the time-series involved in modulating the excitatory and inhibitory components of the emotional arousal response, a result consistent with predicted outputs for a negative feedback loop with unbalanced excitatory and inhibitory components. The coefficients also were significantly correlated with two different types of heart rate variability analyses, providing evidence that the relationships defined by this type of time-series analysis may be physiological meaningful in understanding the interactions between the neural and autonomic components of the emotional arousal response.

REFERENCES

Abboud FM (1982): The sympathetic system in hypertension. State-of-the-art review. Hypertension 4:208–225.

Akselrod S, Gordon D, Ubel FA, Shannon DC, Berger AC, Cohen RJ (1981): Power spectrum analysis of heart rate fluctuation: A quantitative probe of beat-to-beat cardiovascular control. Science 213:220–222.

Bauernschmitt R, Malberg H, Wessel N, Kopp B, Schirmbeck EU, Lange R (2004): Impairment of cardiovascular autonomic control in patients early after cardiac surgery. Eur J Cardiothorac Surg 25:320–326.

Baxter MG, Parker A, Lindner CC, Izquierdo AD, Murray EA (2000): Control of response selection by reinforcer value requires interaction of amygdala and orbital prefrontal cortex. J Neurosci 20:4311–4319.

Berger RD, Akselrod S, Gordon D, Cohen RJ (1986): An efficient algorithm for spectral analysis of heart rate variability. IEEE Trans Biomed Eng 33:900–904.

Blair HT, Sotres-Bayon F, Moita MA, Ledoux JE (2005): The lateral amygdala processes the value of conditioned and unconditioned aversive stimuli. Neuroscience 133:561–569.

Braun C, Kowallik P, Freking A, Hadeler D, Kniffki KD, Meesmann M (1998): Demonstration of nonlinear components in heart rate variability of healthy persons. Am J Physiol 275:H1577–H1584.

Breiter HC, Etcoff NL, Whalen PJ, Kennedy WA, Rauch SL, Buckner RL, Strauss MM, Hyman SE, Rosen BR (1996): Response and habituation of the human amygdala during visual processing of facial expression. Neuron 17:875–887.

Brosschot JF, Van Dijk E, Thayer JF (2006): Daily worry is related to low heart rate variability during waking and the subsequent nocturnal sleep period. Int J Psychophysiol 63:39–47.

Calabresi P, Mercuri NB, De Murtas M, Bernardi G (1991): Involvement of GABA systems in feedback regulation of glutamate-and GABA-mediated synaptic potentials in rat neostriatum. J Physiol 440:581–599.

Cannistraro PA, Rauch SL (2003): Neural circuitry of anxiety: Evidence from structural and functional neuroimaging studies. Psychopharmacol Bull 37:8–25.

Charney DS (2004): Psychobiological mechanisms of resilience and vulnerability: Implications for successful adaptation to extreme stress. Am J Psychiatry 161:195–216.

Chon KH, Zhong Y, Wang H, Ju K, Jan KM (2006): Separation of heart rate variability components of the autonomic nervous system by utilizing principal dynamic modes. Nonlinear Dynamics Psychol Life Sci 10:163–185.

Corcoran KA, Desmond TJ, Frey KA, Maren S (2005): Hippocampal inactivation disrupts the acquisition and contextual encoding of fear extinction. J Neurosci 25:8978–8987.

Critchley HD (2005): Neural mechanisms of autonomic, affective, and cognitive integration. J Comp Neurology 493:154–166.

Critchley HD, Mathias CJ, Josephs O, O'Doherty J, Zanini S, Dewar B-K, Cipolotti L, Shallice T, Dolan RJ (2003): Human cingulate cortex and autonomic control: Converging neuroimaging and clinical evidence. Brain 126:2139–2152.

Davis M, Whalen PJ (2001): The amygdala: Vigilance and emotion. Mol Psychiatry 6:13–34.

Davydov DM, Shapiro D, Cook IA, Goldstein I (2006): Baroreflex mechanisms in major depression. Prog Neuropsychopharmacol Biol Psychiatry 31:164–177.

Donegan NH, Sanislow CA, Blumberg HP, Fulbright RK, Lacadie C, Skudlarski P, Gore JC, Olson IR, McGlashan TH, Wexler BE (2003): Amygdala hyperreactivity in borderline personality disorder: Implications for emotional dysregulation. Biol Psychiatry 54:1284–1293.

Ekman P (1993): Facial expression and emotion. Am Psychol 48:384–392.

Friston KJ (1995): Commentary and opinion. II. Statistical parametric mapping: ontology and current issues. J Cereb Blood Flow Metab 15:361–370.

Goldstein RE, Beiser GD, Stampfer M, Epstein SE (1975): Impairment of autonomically mediated heart rate control in patients with cardiac dysfunction. Circ Res 36:571–578.

Gorman JM, Sloan RP (2000): Heart rate variability in depressive and anxiety disorders. Am Heart J 140 (4 Suppl): 77–83.

Graci S, Baratta R, Degano C, Luppa A, Vigneri R, Frittitta L, Trischitta V (1999): The intravenous insulin tolerance test is an accurate method for screening a general population for insulin resistance and related abnormalities. J Endocrinol Invest 22:472–475.

Hastings RS, Parsey RV, Oquendo MA, Arango V, Mann JJ (2004): Volumetric analysis of the prefrontal cortex, amygdala, and hippocampus in major depression. Neuropsychopharmacology 29:952–959.

Heldman HR (2003): Encyclopedia of Agricultural, Food, and Biological Engineering. New York: Marcel Dekker. 497 p.

Hodgkin AL, Huxley AF (1952): Currents carried by sodium and potassium ions through the membrane of the giant axon of Loligo. J Physiol 116:449–472.

Holt DJ, Titone D, Long LS, Goff DC, Cather C, Rauch SL, Judge A, Kuperberg GR (2006): The misattribution of salience in delusional patients with schizophrenia. Schizophr Res 83:247–256.

Huikuri HV, Makikallio TH (2001): Heart rate variability in ischemic heart disease. Auton Neurosci 90:95–101.

Huikuri HV, Makikallio TH, Perkiomaki J (2003): Measurement of heart rate variability by methods based on nonlinear dynamics. J Electrocardiol 36 (Suppl): 95–99.

Insel PA, Liljenquist JE, Tobin JD, Sherwin RS, Watkins P, Andres R, Berman M (1975): Insulin control of glucose metabolism in man: A new kinetic analysis. J Clin Invest 55:1057–1066.

Izquierdo A, Murray EA (2005): Opposing effects of amygdala and orbital prefrontal cortex lesions on the extinction of instrumental responding in macaque monkeys. Eur J Neurosci 22:2341–2346.

Izquierdo A, Suda RK, Murray EA (2005): Comparison of the effects of bilateral orbital prefrontal cortex lesions and amygdala lesions on emotional responses in rhesus monkeys. J Neurosci 25:8534–8542.

Julius S, Esler MD, Randall OS (1975): Role of the autonomic nervous system in mild human hypertension. Clin Sci Mol Med Suppl 2:243s–252s.

Kandel E, Schwartz J, Jessell T (2000): Principles of Neural Science. New York: The McGraw-Hill.

Kandel ER, Schwartz J, Jessell TM (1991): Principles of Neural Science. Appleton and Lange, Norwalk, CT.

Kaplan Dea. Available at: http://www.macalester.edu/%7Ekaplan/hrv/doc/index.html.

Kernohan AF, Perry CG, Small M (2003): Clinical impact of the new criteria for the diagnosis of diabetes mellitus. Clin Chem Lab Med 41:1239–1245.

Khoo MCK (2000): Physiological Control Systems, Analysis, Simulation and Estimation. New York: Wiley. p 1.

Krasnow B, Tamm L, Greicius MD, Yang TT, Glover GH, Reiss AL, Menon V (2003): Comparison of fMRI activation at 3 and 1.5 T during perceptual, cognitive, and affective processing. Neuroimage 18:813–826.

Kurths J, Voss A, Saparin P, Witt A, Kleiner HJ, Wessel N (1995): Quantitative analysis of heart rate variability. Chaos 5:88–94.

LeDoux JE (2000): Emotion circuits in the brain. Annu Rev Neurosci 23:155–184.

Lombardi F (2002): Clinical implications of present physiological understanding of HRV components. Card Electrophysiol Rev 6:245–249.

Lucas KJ, Karounos DG, Ellis GJ III, Morris MA, Pisetsky DS, Feinglos MN (1986): The intravenous insulin tolerance test in type I diabetes. Res Commun Chem Pathol Pharmacol 53:331–345.

Makikallio TH, Tapanainen JM, Tulppo MP, Huikuri HV (2002): Clinical applicability of heart rate variability analysis by methods based on nonlinear dynamics. Card Electrophysiol Rev 6:250–255.

Malik M, Camm AJ (1993): Components of heart rate variability—What they really mean and what we really measure. Am J Cardiol 72:821–822.

Maren S (2005): Building and burying fear memories in the brain. Neuroscientist 11:89–99.

Marmarelis VZ (1997): Modeling methodology for nonlinear physiological systems. Ann Biomed Eng 25:239–251.

Marmarelis VZ, Chon KH, Holstein-Rathlou NH, Marsh DJ (1999): Nonlinear analysis of renal autoregulation in rats using principal dynamic modes. Ann Biomed Eng 27:23–31.

Marmarelis VZ, Orme ME (1993): Modeling of neural systems by use of neuronal modes. IEEE Trans Biomed Eng 40:1149–1158.

Matthews SC, Paulus MP, Simmons AN, Nelesen RA, Dimsdale JE (2004): Functional subdivisions within anterior cingulate cortex and their relationship to autonomic nervous system function. NeuroImage 22:1151–1156.

Mujica-Parodi LR, Yeragani V, Malaspina D (2005): Nonlinear complexity and spectral analyses of heart rate variability in medicated and unmedicated patients with schizophrenia. Neuropsychobiology 51:10–15.

Nahshoni E, Aravot D, Aizenberg D, Sigler M, Zalsman G, Strasberg B, Imbar S, Adler E, Weizman A (2004): Heart rate variability in patients with major depression. Psychosomatics 45:129–134.

Neumann SA, Brown SM, Ferrell RE, Flory JD, Manuck SB, Hariri AR (2006): Human choline trasporter gene variation is associated with corticolimbin reactivity and autonomic-cholinergic function. Biol Psychiatry 60:1155–1162.

Nomura M, Ohira H, Haneda K, Iidaka T, Sadato N, Okada T, Yonekura Y (2004): Functional association of the amygdala and ventral prefrontal cortex during cognitive evaluation of facial expressions primed by masked angry faces: an event-related fMRI study. Neuroimage 21:352–363.

Phelps EA, Delgado MR, Nearing KI, LeDoux JE (2004): Extinction learning in humans: Role of the amygdala and vmPFC. Neuron 43:897–905.

Phillips ML, Young AW, Senior C, Brammer M, Andrew C, Calder AJ, Bullmore ET, Perrett DI, Rowland D, Williams SC, Gray JA, David AS (1997): A specific neural substrate for perceiving facial expressions of disgust. Nature 389:495–498.

Pomeranz B, Macaulay RJ, Caudill MA, Kutz I, Adam D, Gordon D, Kilborn KM, Barger AC, Shannon DC, Cohen RJ (1985): Assessment of autonomic function in humans by heart rate spectral analysis. Am J Physiol 248 (1 Part 2): H151–H153.

Poon CS, Merrill CK (1997): Decrease of cardiac chaos in congestive heart failure. Nature 389:492–495.

Rolandsson O, Hagg E, Nilsson M, Hallmans G, Mincheva-Nilsson L, Lernmark A (2001): Prediction of diabetes with body mass index, oral glucose tolerance test and islet cell autoantibodies in a regional population. J Intern Med 249:279–288.

Rosenkranz JA, Moore H, Grace AA (2003): The prefrontal cortex regulates lateral amygdala neuronal plasticity and responses to previously conditioned stimuli. J Neurosci 23:11054–11064.

Schafer A, Schienle A, Vaitl D (2005): Stimulus type and design influence hemodynamic responses towards visual disgust and fear elicitors. Int J Psychophysiol 57:53–59.

Schienle A, Schafer A, Walter B, Stark R, Vaitl D (2005): Brain activation of spider phobics towards disorder-relevant, generally disgust- and fear-inducing pictures. Neurosci Lett 388:1–6.

Schwartz PJ, De Ferrari GM (1987): The influence of the autonomic nervous system on sudden cardiac death. Cardiology 74:297–309.

Shin LM, Wright CI, Cannistraro PA, Wedig MM, McMullin K, Martis B, Macklin ML, Lasko NB, Cavanagh SR, Krangel TS, Orr SP, Pitman RK, Whalen PJ, Rauch SL (2005): A functional magnetic resonance imaging study of amygdala and medial prefrontal cortex responses to overtly presented fearful faces in posttraumatic stress disorder. Arch Gen Psychiatry 62:273–281.

Smith SM (2002): Fast robust automated brain extraction. Hum Brain Mapp 17:143–155.

Somerville LH, Kim H, Johnstone T, Alexander AL, Whalen PJ (2004): Human amygdala responses during presentation of happy and neutral faces: Correlations with state anxiety. Biol Psychiatry 55:897–903.

Sotres-Bayon F, Bush DE, LeDoux JE (2004): Emotional perseveration: An update on prefrontal-amygdala interactions in fear extinction. Learn Mem 11:525–535.

Sotres-Bayon F, Cain CK, Ledoux JE (2006): Brain mechanisms of fear extinction: Historical perspectives on the contribution of prefrontal cortex. Biol Psychiatry 60:329–336.

Spielberger CD (1983): Manual for the State-Trait Anxiety Inventory (Form Y). Palo Alto, CA: Consulting Psychologists Press.

Sriussadaporn S, Ploybutr S, Peerapatdit T, Plengvidhya N, Nitiyanant W, Vannasaeng S, Vichayanrat A (1996): Nocturnal 8 mg dexamethasone suppression test: A practical and accurate test for identification of the cause of endogenous Cushing's syndrome. Br J Clin Pract 50:9–13.

Swynghedauw B, Jasson S, Chevalier B, Clairambault J, Hardouin S, Heymes C, Mangin L, Mansier P, Medigue C, Moalic JM, Thibault N, Carré F (1997): Heart rate and heart rate variability, a pharmacological target. Cardiovasc Drugs Ther 10:677–685.

Task Force of the European Society of Cardiology and the North American Society of Pacing and Electrophysiology (1996): Heart rate variability: Standards of measurement, physiological interpretation and clinical use. Circulation 93:1043–1065.

Tyrrell JB, Findling JW, Aron DC, Fitzgerald PA, Forsham PH (1986): An overnight high-dose dexamethasone suppression test for rapid differential diagnosis of Cushing's syndrome. Ann Intern Med 104:180–186.

van der Kooy KG, van Hout HP, van Marwijk HW, de Haan M, Stehouwer CD, Beekman AT (2006): Differences in heart rate variability between depressed and non-depressed elderly. Int J Geriatr Psychiatry 21:147–150.

Ventura J, Liberman RP, Green MF, Shaner A, Mintz J (1998): Training and quality assurance with the structured clinical interview for DSM-IV (SCID-I/P). Psychiatry Res 79:163–73.

Vigo DE, Nicola SL, Ladron de Guevara MS, Martinez-Martinez JA, Fahrer RD, Cardinali DP, Masoli O, Guinjoan SM (2004): Relation of depression to heart rate nonlinear dynamics in patients > or = 60 years of age with recent unstable angina pectoris or acute myocardial infarction. Am J Cardiol 93:756–760.

Voss A, Kurths J, Kleiner HJ, Witt A, Wessel N. (1995): Improved analysis of heart rate variability by methods of nonlinear dynamics. J Electrocardiol 28 (Suppl): 81–88.

Voss A, Kurths J, Kleiner HJ, Witt A, Wessel N, Saparin P, Osterziel KJ, Schurath R, Dietz R (1996): The application of methods of non-linear dynamics for the improved and predictive recognition of patients threatened by sudden cardiac death. Cardiovasc Res 31:419–433.

Wessel N, Voss A, Malberg H, Ziehmann Ch, Voss HU, Schirdewan A, Meyerfeldt U, Kurths J (2000): Nonlinear analysis of complex phenomena in cardiological data. Herzschr Elektrophys 11:159–173.

Wilhelm FH, Trabert W, Roth WT (2001): Physiologic instability in panic disorder and generalized anxiety disorder. Biol Psychiatry 49:596–605.

Williams LM, Das P, Harris AW, Liddell BB, Brammer MJ, Olivieri G, Skerrett D, Phillips ML, David AS, Peduto A, Gordon E (2004): Dysregulation of arousal and amygdala-prefrontal systems in paranoid schizophrenia. Am J Psychiatry 161:480–489.

Yeragani VK, Pohl R, Balon R, Ramesh C, Glitz D, Jung I, Sherwood P (1991): Heart rate variability in patients with major depression. Psychiatry Res 37:35–46.

Yeragani VK, Sobolewski E, Igel G, Johnson C, Jampala VC, Kay J, Hillman N, Yeragani S, Vempati S (1998): Decreased heart-period variability in patients with panic disorder: A study of Holter ECG records. Psychiatry Res 78:89–99.

Zhong Y, Jan KM, Ju KH, Chon KH (2006): Quantifying cardiac sympathetic and parasympathetic nervous activities using principal dynamic modes analysis of heart rate variability. Am J Physiol Heart Circ Physiol 291:H1475–H1483.

Zhong Y, Wang H, Ju KH, Jan KM, Chon KH (2004): Nonlinear analysis of the separate contributions of autonomic nervous systems to heart rate variability using principal dynamic modes. IEEE Trans Biomed Eng 51:255–262.